Behavioral/Systems/Cognitive

Role of Afferents in the Differentiation of Bipolar Cells in the Mouse Retina

Patrick W. Keeley[1,3] **and Benjamin E. Reese**[2,3]

Departments of [1]Molecular, Cellular, and Developmental Biology and [2]Psychology, and [3]Neuroscience Research Institute, University of California at Santa Barbara, Santa Barbara, California 93106

To establish dendritic arbors that integrate properly into a neural circuit, neurons must rely on cues from the local environment. The neurons presynaptic to these arbors, the afferents, are one potential source of these cues, but the particular dendritic features they regulate remain unclear. Retinal bipolar cells can be classified by the type of photoreceptor, cone or rod, forming synaptic contacts with their dendrites, suggesting a potential role of these afferents in shaping the bipolar cell dendritic arbor. In the present investigation, the role of photoreceptors in directing the differentiation of bipolar cells has been studied using two genetically modified "coneless" and "conefull" mice. Single cone (Type 7/CB4a) and rod bipolar cells were labeled with DiI to reveal the entire dendritic arbor and subsequently analyzed for several morphological features. For both cone and rod bipolar cells, the dendritic field area, number of dendritic terminals, and stratification of terminals in the outer plexiform layer were comparable among coneless, conefull, and wild-type retinas, and the overall morphological appearance of each type of cell was essentially conserved, indicating an independence from afferent specification. The presence of normal afferents was, however, found to be critical for the proper spatial distribution of dendritic terminals, exhibiting a clustered distribution for the cone bipolar cells and a dispersed distribution for the rod bipolar cells. These results demonstrate a selectivity in the afferent dependency of bipolar cell differentiation, their basic morphogenetic plan commanded cell intrinsically, and their fine terminal connectivity directed by the afferents themselves.

Introduction

Dendritic morphogenesis is facilitated by a combination of cell intrinsic and environmental factors, yet how exactly these factors affect individual aspects of the dendritic arbor remains unknown. The retina provides a model system to address this problem, because many characteristics of these arbors can be parsed and measured, including dendritic spread, stratification, and branching, allowing for the factors responsible for establishing each of these features to be elucidated. Regulation of dendritic spread, for example, is known to be dependent on homotypic interactions for some cell types [e.g., the retinal horizontal cell (Reese et al., 2005; Poché et al., 2008)], although other types appear to be immune to this form of regulation [e.g., the cholinergic amacrine cell (Farajian et al., 2004; Keeley et al., 2007); the dopaminergic amacrine cell (Keeley and Reese, 2010)]. Homotypic interactions are not the only environmental cues that shape dendritic arbors; afferents also may play a role, through the expression of cell recognition molecules, release of trophic factors, transmission of visual activity, or a combination of such mechanisms. For instance, the stratification of certain ganglion cell arbors in the inner plexiform layer (IPL) relies on visual activity (Tian and Copenhagen, 2003), modulated through BDNF–TrkB signaling (Liu et al., 2007). Cell adhesion molecules in the retina have also been suggested to play a role (Yamagata and Sanes, 2008), promoting homophilic binding between afferents and targets. Distinguishing the source of these cues, however, is complicated because of the complex and poorly understood connectivity between many different subtypes of ganglion cells, bipolar cells, and amacrine cells in the IPL. Alternatively, exploring the afferent control of dendritic morphogenesis in the outer plexiform layer (OPL) is straightforward, by comparison, because it contains only two sources of afferents, the cone and rod photoreceptors. In this study, we investigated the role of these afferents on bipolar cell morphogenesis.

Retinal bipolar cells can be divided into two major classes: nine types of cone bipolar cell and one type of rod bipolar cell (Ghosh et al., 2004, Pignatelli and Strettoi, 2004), being postsynaptic to the cones and rods, respectively (but see Tsukamoto et al., 2001; Mataruga et al., 2007; Haverkamp et al., 2008). During development, the photoreceptor terminals arrive in the OPL in advance of bipolar cell differentiation (Rich et al., 1997; Sherry et al., 2003; Morgan et al., 2006), thereby being positioned, both spatially and temporally, to influence the growth of these bipolar processes. The dendrites of bipolar cells have also been shown to remodel after photoreceptor degeneration (Strettoi et al., 2003; Haverkamp et al., 2006), consistent with the idea that dendritic morphology is dependent on afferent input. Those latter studies, however, demonstrate only an afferent dependency for the maintenance of dendritic morphology, not the initial acquisition of

Received Oct. 14, 2009; revised Dec. 9, 2009; accepted Dec. 16, 2009.

This research was supported by National Institutes of Health Grants EY-11087 and RR-22585. We thank Dr. Mary Raven for her assistance with the spatstat software package, Drs. Richard Masland and Bin Lin for providing the Gustducin–GFP transgenic mice, Dr. Anand Swaroop for providing the *Nrl*$^{-/-}$ mice, and Dr. Jeremy Nathans for providing the coneless transgenic mice.

Correspondence should be addressed to Benjamin E. Reese, Neuroscience Research Institute, University of California, Santa Barbara, CA 93106-5060. E-mail: breese@psych.ucsb.edu.

DOI:10.1523/JNEUROSCI.5153-09.2010

 0270-6474/10/301677-09$15.00/0

that morphology. To assess this possible role for afferent specification of dendritic morphogenesis, we have analyzed the dendritic arbors of bipolar cells in two genetically engineered mouse lines in which the composition of the outer nuclear layer is altered during early development, being the "coneless" mutant mouse and the "conefull" $Nrl^{-/-}$ mouse.

Materials and Methods

Breeder pairs of the Gustducin–green fluorescent protein (GFP) mouse line, in which an 8.4 kb segment upstream of the α-gustducin gene drives the expression of GFP in retinal bipolar cells (Huang et al., 2003), were obtained and bred in the Animal Resource Center at the University of California at Santa Barbara (UCSB). Offspring were crossed with two other genetically engineered mouse lines, the coneless and the conefull mice. In coneless mice, a human L-cone opsin promoter sequence drives an attenuated diphtheria toxin transgene that subsequently kills off 95% of the cones in early development (Soucy et al., 1998; Raven and Reese, 2003). In the conefull mouse, the *neural retina leucine zipper* (*Nrl*) gene is knocked out, causing all photoreceptors to adopt the cone fate (Mears et al., 2001). Because both copies of the *Nrl* gene must be knocked out to achieve the desired phenotype, GFP-positive, *Nrl* heterozygotes from the F1 progeny were crossed to produce GFP-positive, *Nrl* knock-outs. GFP-positive littermates that did not have the genotype of interest were used as wild-type (WT) controls for each condition. Both engineered lines are on a C57BL/6 background, but the coneless line is on a mixed background of C57BL/6J and C57BL/6Ncrl. Because these two lines are essentially substrains now known to differ in the density of other retinal cell types (Whitney et al., 2009), we have included WT littermate controls for each comparison and analyzed them separately. Adult mice were used in all analyses, having an average ± SD postnatal age of 72 ± 14 d. All experiments were conducted under authorization by the Institutional Animal Care and Use Committee at UCSB and in accord with the National Institutes of Health *Guide for the Care and Use of Laboratory Animals*.

DiI labeling. Mice were euthanized with sodium pentobarbital (120 mg/kg, i.p.), and eyes were immersion fixed in 4% paraformaldehyde for 30 min. Whole retinas were dissected immediately, rinsed in sodium phosphate buffer, and transferred to an injection-well mounted on a fixed stage Nikon Eclipse E600 microscope. A single GFP-positive bipolar cell axon terminal in one of the two distinct strata in the IPL (Fig. 1*b*) was visualized and impaled with a micropipette filled with 0.5% DiI in 100% EtOH solution. A small amount of DiI was deposited by passing positive current through the pipette for ~10 s, at which point the dye could be seen spreading locally within the membrane of the injected terminal in the IPL (and subsequently left overnight, this lipophilic dye continues to diffuse throughout the entire membrane of the cell). After injecting multiple cells in this manner across the retina, some retinas were subsequently labeled with peanut agglutinin (PNA) conjugated with the fluorochrome Alexa Fluor 647 (PNA–AF647; 1:500; catalog #L-32460; Invitrogen) in PBS overnight to label the active sites of cone pedicles (Haverkamp et al., 2001). GFP-positive, DiI-labeled somata and dendritic fields were imaged within 48 h using an Olympus Fluoview 500 laser scanning confocal microscope with a 60× oil-immersion objective at 0.5 μm intervals through the *z*-axis. Captured image stacks were deconvoluted and analyzed using AutoQuant version X1.4.1 (Media Cybernetics) and MetaMorph version 7.5.4.0 (MDS Analytical Technologies) software, respectively. Some retinas that had been labeled for DiI as above were subsequently sectioned at 150 μm on a Vibratome (The Vibratome Company) to examine their dendritic morphology in the radial axis.

Immunofluorescence. GFP-positive retinas were also prepared for immunofluorescence. Retinas were embedded in 5% agarose and cut into radial sections at a thickness of 150 μm on a Vibratome. Sections were stained with PNA–AF647 (1:1000), mouse monoclonal antibodies to C-terminal binding protein 2 (CtBP2) (1:250; catalog #612044; BD Biosciences), and either rabbit polyclonal antibodies to protein kinase C (PKC) (1:10,000; catalog #CA-1042; Cambio) or rabbit polyclonal antibodies to GFP conjugated to Alexa Fluor 488 (GFP–AF488; 1:1000; catalog #A-21311; Invitrogen) by using the following protocol: sections were rinsed in phosphate buffer, preincubated in 5% normal donkey serum and 1% Triton X-100 in PBS for 3 h, and then rinsed with PBS. Sections were then incubated with agitation for 3 d at 4°C in the primary antibodies and PNA–AF647 plus 1% Triton X-100 in PBS. Retinas were rinsed in PBS and stained overnight with donkey anti-mouse secondary IgG conjugated to cyanine 3 (1:200; catalog #715-165-150; Jackson ImmunoResearch) and donkey anti-rabbit secondary IgG conjugated to AF488 (1:200; catalog #A21206; Invitrogen) to detect CtBP2 and PKC primary antibodies, respectively. Sections were imaged using an Olympus Fluoview 1000 laser scanning confocal microscope with a 40× water-immersion objective, sampling images at 1 μm intervals.

Morphometrics. Whole-mount image stacks of DiI-labeled bipolar cells were measured for the following characteristics: dendritic field area, soma area, terminal number, and terminal location in the *x–y* plane.

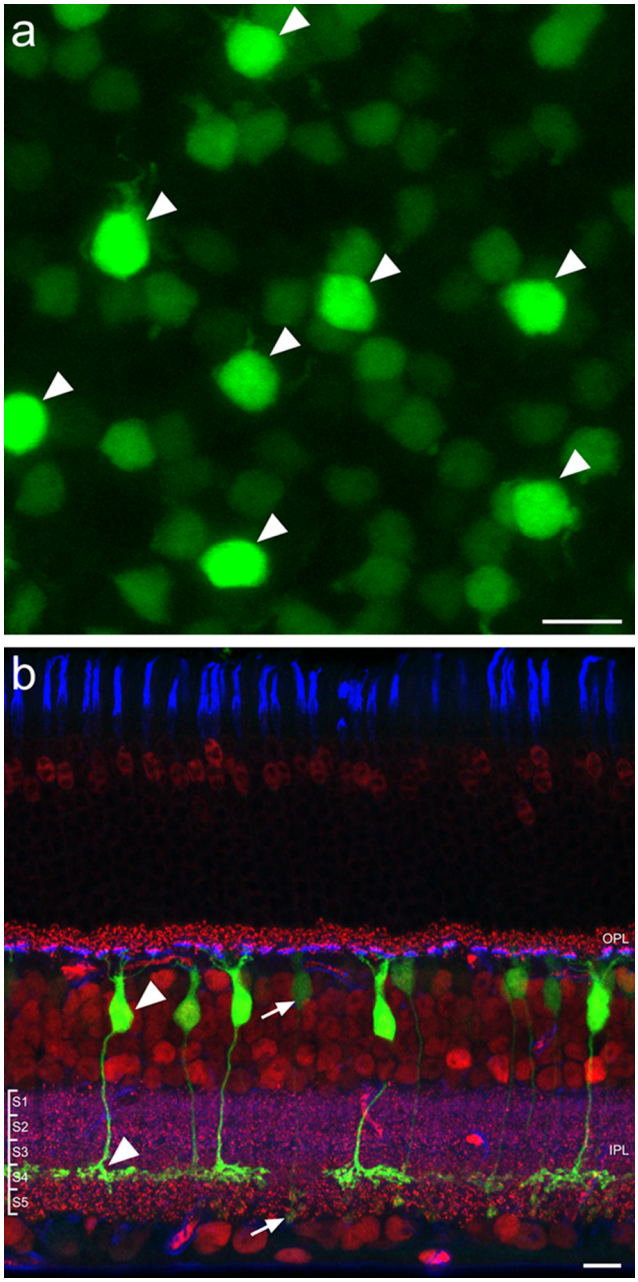

Figure 1. GFP-positive cells (green) can be discriminated by the intensity of their fluorescence (***a***) and by their stratification in the IPL (***b***). The brighter cells (arrowheads) stratify in S4 of the IPL and are a single type of cone bipolar cell (Type 7 as classified by Ghosh et al., 2004; type CB4a as classified by Pignatelli and Strettoi, 2004), and the fainter cells (arrows in ***b***) stratify in S5 of the IPL and are the rod bipolar cells. CtBP2 (red) and PNA (blue) were used to identify the boundaries of the IPL and OPL. Scale bars, 10 μm.

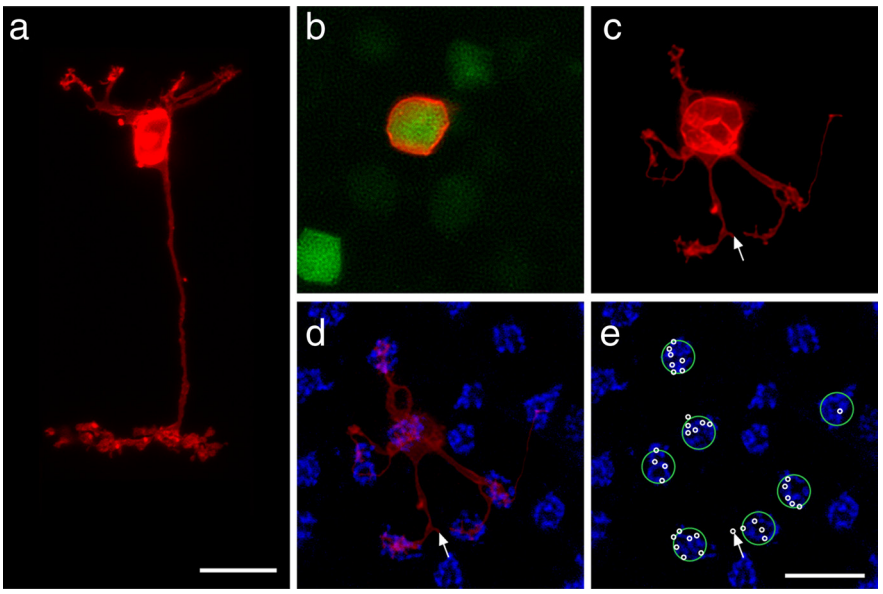

Figure 2. Single DiI-labeled (red) GFP-positive (green) cone bipolar cells from wild-type retinas, shown in radial section (***a***) and in whole-mount sampled from the soma (***b***) through the OPL (***c–e***). The cell in ***a*** had been labeled in section, by injecting the soma, whereas the cell in ***b*** had been labeled by injecting the axon arbor in the IPL. Notice individual dendrites radiating out from the soma, branching to form discrete clusters of terminals. These terminal clusters are invariably associated with the presence of active sites at cone pedicles, revealed by PNA labeling (blue, ***d***, ***e***). Individual pedicles contacted by this bipolar cell are indicated by large green circles, and the locations of individual terminals are indicated by small white circles (***e***). Also note a terminal found some distance from all neighboring cone pedicles (arrow). Scale bars, 10 μm.

Dendritic field area was determined by finding the area of the convex polygon that surrounded the dendrites of each cell; likewise, soma area was calculated by tracing the cell body at its widest extent. Terminals were defined as the tip of any dendritic branch. To analyze the spatial patterning of dendritic terminals in the plane of the retina, the *x–y* coordinates of each terminal was used to compute the Delaunay triangulation of the dendritic field by using the spatstat package (www.spatstat.org) in the programming language R (www.r-project.org). The coefficient of variation was determined for each cell by dividing the SD by the mean Delaunay triangle area. Student's *t* tests were used for each comparison with $p < 0.01$ determining significance.

Sections of GFP-positive cone bipolar cells were analyzed for the depth at which their branches terminated in the OPL. The boundary of the OPL, defined using CtBP2-labeled ribbon synapses, and the locations of each discernable terminal were recorded independently. Once the terminal locations were overlaid on the OPL boundary, depth was measured as the distance of the terminal relative to the distance of a line drawn radially through the terminal from the inner to outer boundary of the OPL.

Results

As described previously by others, we found GFP expression to be limited to one class of cone bipolar cell and the single class of rod bipolar cell, each expressing at a different intensity (Fig. 1*a*) that allowed for the cells to be discriminated consistently (Huang et al., 2003; Lin and Masland, 2005): every brightly labeled GFP-positive bipolar cell extended a terminal into S4 of the IPL (Fig. 1*b*, arrowheads) and, when subsequently labeled with DiI, had a cone bipolar morphology (Fig. 2*a*), whereas every faintly labeled GFP-positive cell extended a terminal into S5 (Fig. 1*b*, arrows) and had a rod bipolar morphology (see Fig. 7*a*). Based on the level of terminal stratification in the IPL, we agree with previous reports (Huang et al., 2003; Lin and Masland, 2005; Wässle et al., 2009) that the gustducin-positive cone bipolar cell most resembles the Type 7/CB4a bipolar cell as classified by Ghosh et al. (2004) and Pignatelli and Strettoi (2004), respectively.

Cone bipolar cell morphology

The entire morphology of this Type 7/CB4a cone bipolar cell is particularly well illustrated in a fortuitous section in which attempts to label the cell from the soma had proven successful (this approach frequently labeled other nearby bipolar cells as well, obscuring the detailed dendritic morphology of the targeted cell): dendritic branches emerge from the soma and splay out as they ascend to the OPL, in which each gives rise to a cluster of fine terminal-like extensions (Fig. 2*a*). A single basally directed process descends radially through the inner nuclear layer (INL) and IPL to reach S4, in which a terminal arbor extends laterally ~30 μm, being comparable with the width of the dendritic arbor. Bipolar axon arbors are generally thought to produce a tiling of their respective strata rather than exhibiting any overlap (Young and Vaney, 1991; Chan et al., 2001; Telkes et al., 2008), and, consistent with this, we rarely obtained more than a single labeled Type 7/CB4a cone bipolar cell when targeting the terminal arbor in whole-mount preparations (Fig. 2*b*).

The clusters of dendritic terminals produced by these bipolar cells are restricted to the innermost portion of the OPL (Fig. 2*c*), in which cone pedicles are known to stratify. By labeling these same retinas to reveal the presence of cone pedicle active sites using PNA (Fig. 2*d*), we confirmed that every dendrite yielding clusters of terminals was associated with a cone pedicle (Fig. 2*e*, green circles), being the invaginating processes of this type of On cone bipolar cell (Mariani, 1981; Hopkins and Boycott, 1996). Occasionally, single terminal-like extensions were positioned away from any pedicles (Fig. 2*c–e*, arrow), which may be associated with rod spherules (Tsukamoto et al., 2007). Notice that individual dendrites do not always grow out to innervate the pedicles directly from the soma; some take conspicuous turns toward the pedicle, whereas other pedicles are innervated by branches from other clusters (Fig. 2*c*,*d*). Note as well that not all pedicles near the soma are innervated. The cell in Figure 2*d* contacts seven different pedicles but spares one nearby the soma. The average ± SD number of pedicles contacted by single Type 7/CB4a cone bipolar cells was 8.7 ± 2.06 based on a sample of 15 single-labeled cells from wild-type retinas that were also labeled for PNA. This estimate confirms that from another recent study reporting 8.4 pedicles contacted by Type 7/CB4a cells (Wässle et al., 2009).

The individual number of terminals per pedicle can also be counted in such specimens. The average ± SD was 3.7 ± 1.68, but this number varied conspicuously depending on the proximity of the pedicle to the main dendritic stalk, when evidenced by pooling the data from these 15 labeled cells (supplemental Fig. 1, available at www.jneurosci.org as supplemental material), and is consistent with evidence from the primate retina (Boycott and Wässle, 1991; Hopkins and Boycott, 1997). Near the stalk, some pedicles had as many as seven or eight terminals, whereas those farther removed from the stalk had as few as one or two. Those latter pedicles should be innervating a second Type 7/CB4a cell,

because Wässle et al. (2009) have shown that pedicles on the fringe of the dendritic field are often connecting to two cone bipolar cells of the same type.

Figure 3, *a* and *c*, illustrates 10 different examples of cone bipolar cells from a larger sample of 95 labeled cells from wild-type retinas and shows, for comparison, five examples from coneless retinas (*b*) and five examples from conefull retinas (*d*). What is immediately striking about these bipolar cells is how relatively normal they appear: like those in the wild-type retinas, bipolar cells in both the coneless and conefull retinas exhibit a comparable divergence of primary dendrites within the OPL, establishing a dendritic field that is similar in size to that observed in the wild-type retinas (Fig. 4*a*). These cone bipolar cells show no gross morphological atrophy of the dendritic arbor in the absence of nearly all cone pedicles (Fig. 3*b*), nor any evidence of conspicuous hypertrophy in the presence of excess numbers of cones (Fig. 3*d*). Soma size was also unaltered (Fig. 4*b*).

A closer examination of individual cone bipolar cells, however, reveals pronounced differences in the detailed connectivity associated with these cells. Although cone bipolar cells in both the coneless and conefull retina established a similar number of terminals as those in wild-type retinas (Fig. 4*c*), they generally failed to exhibit discrete clusters of terminals (Fig. 5*a*,*e* and *d*,*h*; compare with Fig. 2*e*) (for the plots of individual terminals for each cell illustrated in Fig. 3, see supplemental Fig. 2, available at www.jneurosci.org as supplemental material). This relative lack of clustering is readily apparent when comparing the Delaunay triangulation associated with the positioning of these terminals within the dendritic field (Fig. 4*d*). The clustered presence of terminals increases the variability in triangle size, and so the coefficient of variation is significantly greater in the wild-type controls relative to either the coneless or conefull retinas (Fig. 4*e*).

The role of pedicles on the positioning of dendritic terminal endings was particularly striking in coneless retinas in which single DiI-labeled, GFP-positive bipolar cells were found near a surviving cone pedicle. Such bipolar cells always showed a discrete cluster of terminals associated with single PNA-labeled active sites compared with the general absence of this clustering phenotype at the termination sites of other primary dendrites (Fig. 5*b*,*f*). Note in some cases that multiple primary dendrites appear to converge on

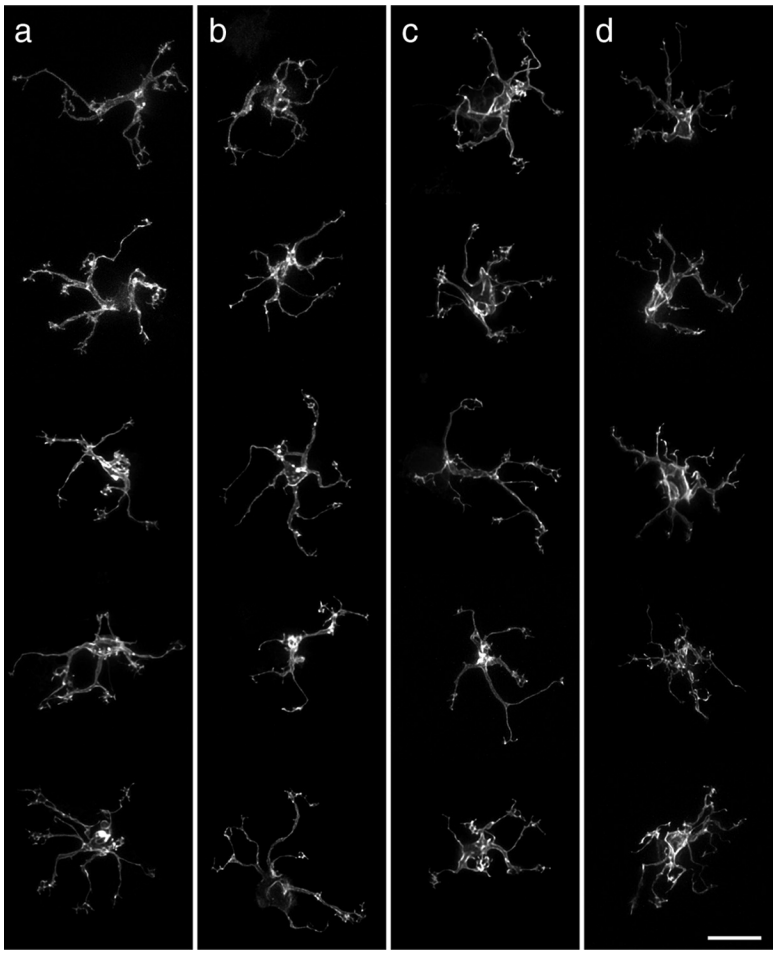

Figure 3. Examples of five cone bipolar cell dendritic fields (the image stacks having been truncated at the INL to remove the somata, for better visualization) from wild-type and coneless littermates (***a***, ***b***) and from wild-type and conefull littermates (***c***, ***d***). The coarse dendritic branching pattern is relatively comparable in the three conditions. Scale bar, 10 μm.

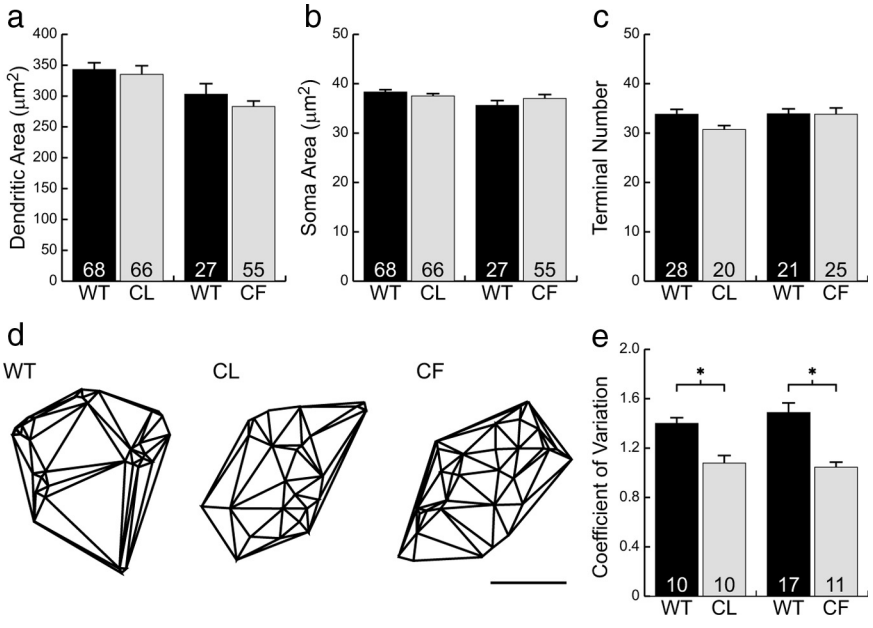

Figure 4. Neither cone bipolar cell dendritic field size (***a***), soma size (***b***), nor terminal branch number (***c***) were significantly different from wild type in either the coneless (CL) or conefull (CF) retinas. The Delaunay triangulation of the dendritic field (***d***) showed those in the wild-type retina to be significantly more clustered than those in either the coneless or conefull retinas (***e***). Means and SEs are plotted in each histogram. Scale bar, 10 μm. *$p < 0.01$.

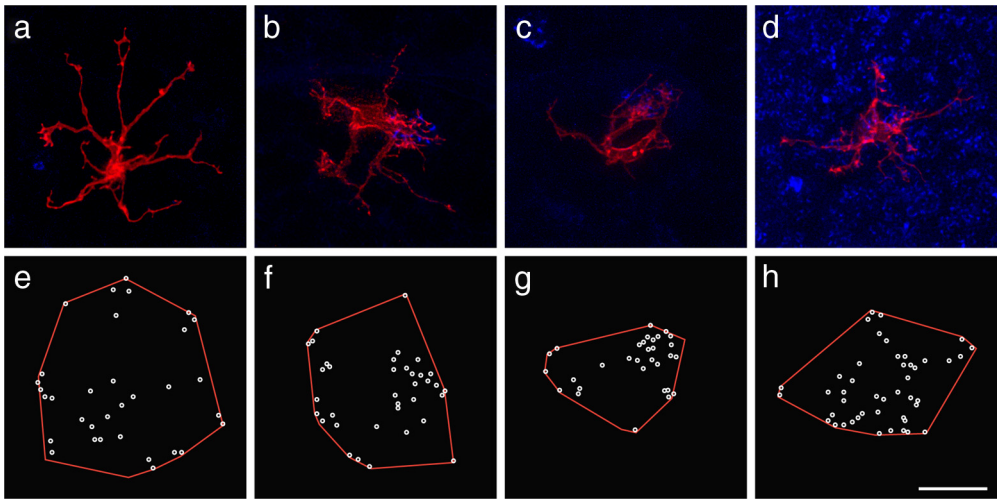

Figure 5. Single cone bipolar cells (red) in coneless (***a–c***) and conefull (***d***) retinas also labeled for PNA (blue), to show examples of cells differentiating in the absence of all cones (***a***) or in the presence of one cone (***b***, ***c***) or in the presence of excess cones (***d***). Plots of dendritic fields in red and the end of each terminal branch in white are shown for each cell (***e–h***). Scale bar, 10 μm.

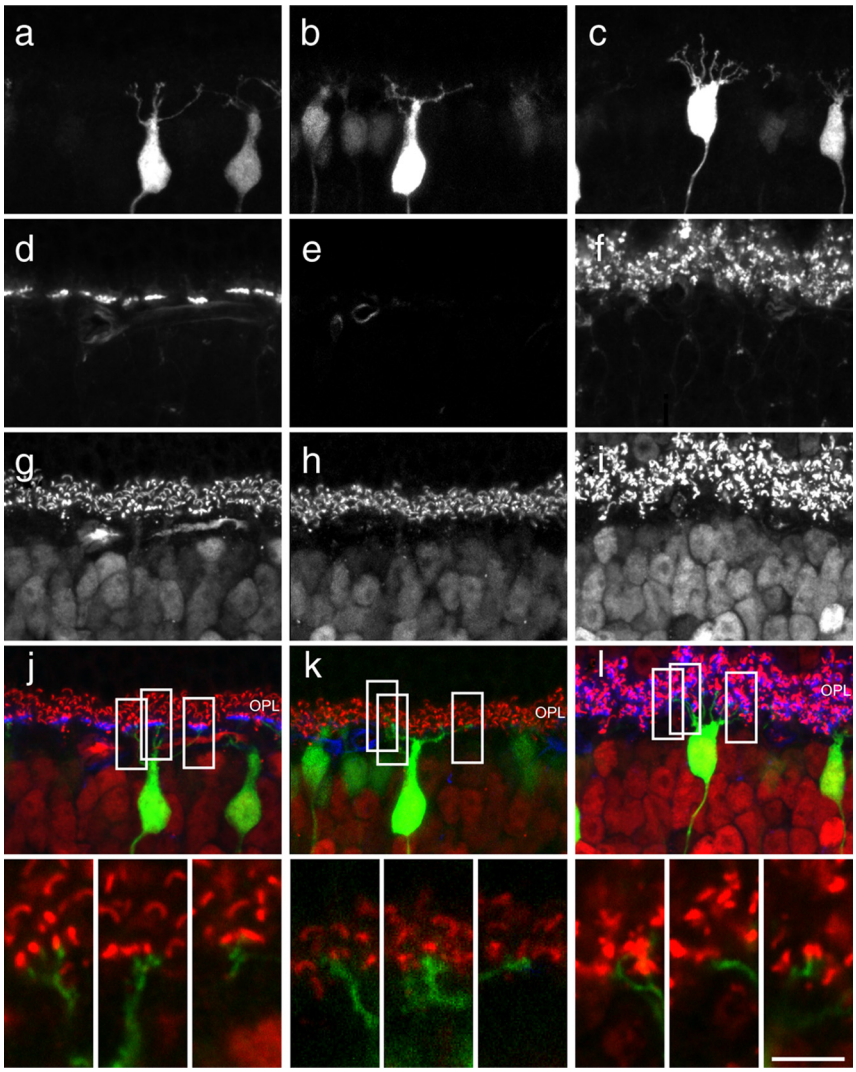

Figure 6. Sections of GFP-positive cone bipolar cells in wild-type, coneless, and conefull retinas (***a–c***) stained for cone pedicles with PNA (***d–f***) and synaptic ribbons with CtBP2 (***g–i***), to reveal the depth of terminal stratification in the OPL (***j–l***). Insets show single 0.5 μm optical sections from different depths of the single *Z*-stack reconstructions in ***j–l*** that reveal dendrites terminating in close proximity to ribbon synapses in all conditions. Notice that cone pedicles are normally restricted to the innermost portion of the OPL (***a***,***d***,***g***,***j***). The GFP-positive dendrites target the inner portion of the OPL in the coneless (***b***,***e***,***h***) as well as conefull (***c***,***f***,***i***) retinas. GFP, CtBP2, and PNA channels are displayed as green, red, and blue in merged images, but only the GFP and CtBP2 are shown at higher magnification in the insets at the bottom. Scale bar: full images, 15 μm; insets, 5 μm.

the same remaining pedicle (Fig. 5*c*,*g*), but, in general, these "partially coneless" cells had dendritic fields that were comparable in size: these cells had dendritic fields that averaged 369 ± 132 μm^2 (SD), whereas "fully coneless" cells averaged 348 ± 136 μm^2 (SD) based on samples of 12 and 20 cells, respectively.

In the conefull retina, PNA labeling no longer reveals a distribution of cone pedicle active sites at the inner margin of the OPL; rather, the entire OPL is now filled with PNA, similar to the widespread presence of cone arrestin (Raven et al., 2007), as would be expected if all of the rods had now differentiated as cones (Fig. 6*f*, compare with *d*, *e*), yet these cones do not produce structures that appear as discrete pedicles with a stratified collection of ribbons at their basal surface (Strettoi et al., 2004), not even at the inner limit of the OPL (Raven et al., 2007). Therefore, the PNA labeling no longer provides a clear landmark for identifying individual pedicles (Fig. 6*f*), and, consequently, it is difficult to associate the dendritic terminals to single pedicles. Nevertheless, it is apparent that bipolar cells in these retinas do not concentrate their terminations at specific locations as do those in wild-type retinas (Figs. 3*d*, 4*d*); instead, they appear to sprout sporadically across the dendritic field, with fewer dendrites elaborating into terminal clusters (Fig. 5*d*, *h*) (supplemental Fig. 2*d*, available at www.jneurosci.org as supplemental material). Interestingly, although these cone bipolar cells extend slightly farther than they normally would (Fig. 6*c*,*f*,*i*,*l*), they fail to invade the more outer reaches of the OPL, that portion of the OPL normally supplied by rod spherules but now colonized by re-

specified cone terminals (supplemental Fig. 3, available at www.jneurosci.org as supplemental material). Indeed, single DiI-labeled cone bipolar cells in radial sections confirm this general impression, that their arbors are only slightly more widespread across the depth of the OPL relative to those in wild-type retinas (supplemental Fig. 4, available at www.jneurosci.org as supplemental material).

Although we can be certain that those clustered terminals in the wild-type retina truly reflect the postsynaptic sites associated with cone innervation, we are less confident about such terminations in the coneless and conefull retina. Given the limitations of our technique, we could not combine DiI labeling with most immunolabeling protocols to juxtapose, at high-resolution, the dendritic terminals with other elements of the OPL; however, when sections of GFP-positive cone bipolar cells were labeled for the presence of photoreceptor ribbon synapses, dendritic terminals were found in close proximity to these ribbons in all conditions (Fig. 6*j–l*), suggesting that, in the coneless retina (Fig. 6*k*), these cone bipolar cells may be making contacts with the remaining rod spherules.

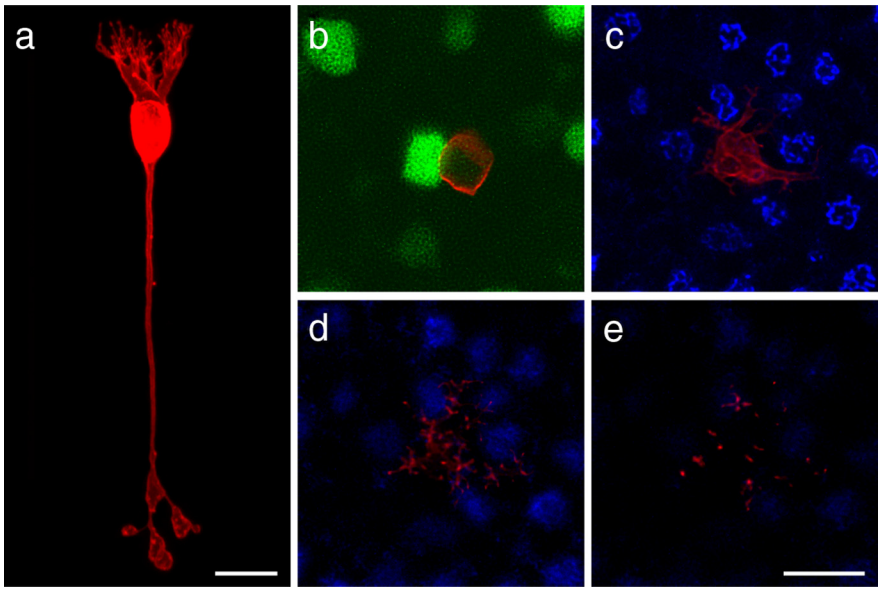

Figure 7. Single DiI-labeled (red) GFP-positive (green) rod bipolar cells from wild-type retinas, shown in radial section (***a***) and in whole mount (***b***). Beginning at the level of the cone pedicles, three consecutive projections, each of 3 μm image stacks, shows that dendritic terminals can be found in all three levels of the OPL but never at the active sites of cone pedicles (***c–e***). Cone pedicles were revealed by labeling with PNA (blue). Scale bars, 10 μm.

Rod bipolar cell morphology

Rod bipolar cells, in contrast with these cone bipolar cells, produce a strikingly distinctive morphology. The rod bipolar cell produces a stout primary dendritic stalk that climbs to the OPL, in which it quickly divides into multiple branches that continue a primarily radial trajectory (Fig. 7*a*), giving rise to a large collection of terminal endings that has limited lateral spread but extends through the full thickness of the OPL (Fig. 7*b–e*), bypassing the population of cone pedicles (Fig. 7*c*) at the inner limit of the OPL. Figure 8, *a* and *c*, shows 10 examples of such single rod bipolar cell dendritic arbors from whole-mounted wild-type retinas presented as *Z*-stack reconstructions through the full depth of the OPL. Rod bipolar cells in the coneless retina are, not surprisingly, comparable with those in the wild-type retinas (Fig. 8, compare *b* with *a*). In the conefull retinas, however, their basic morphology was not conspicuously altered in these preparations, certainly not being atrophic in the absence of the rods (Fig. 8, compare *d* with *c*). Neither dendritic field area nor soma size was significantly different in the two experimental conditions (Fig. 9*a*,*b*), and nor was the total number of individual terminals throughout the full depth of the dendritic field altered (Fig. 9*c*). These morphometric analyses confirm the observations of others using the $Nrl^{-/-}$ mouse (Strettoi et al., 2004) on the basis of PKC immunoreactivity.

We did notice, however, that dendritic tips in wild-type and coneless rod bipolar cells end in bulbous terminations, interpreted as the expansion of these processes after they pass through the neck of the invagination at the basal surface of the spherule (Grünert and Martin, 1991). Labeled cells in the conefull retina failed to display such conspicuous puncta at the ends of the dendritic terminals (Fig. 8, compare *d* with *a–c*). Such terminals are located adjacent to PNA-labeled active sites and ribbon synapses in the conefull retina (Fig. 10*c*,*f*,*i*,*l*) and are believed to invaginate the respecified cones in these retinas, because the terminals of the latter have been shown to exhibit invaginating elements thought to come from the rod bipolar cells (Strettoi et al., 2004).

Closer examination revealed that the primary dendritic stalks of the rod bipolar cells in conefull retinas were notably coarser and extended for a greater distance from the soma into the OPL (Fig. 10*c*). This was confirmed by comparing single DiI-labeled rod bipolar cells in sectioned conefull versus wild-type retinas (supplemental Fig. 5, available at www.jneurosci.org as supplemental material). These images, like those in the PKC-labeled specimens in Figure 10*c*, suggest that the distribution of terminal endings might be less evenly distributed within the OPL. To assess this, we identified the *x*,*y* positions of each dendritic terminal for multiple labeled cells in whole-mount preparations and conducted a comparable analysis of clustering (Fig. 9*d*). Although this approach ignores all *z*-axis variation, it shows rather clearly that the distribution of terminations for single rod bipolar cells is perturbed in the conefull retina relative to the wild-type and coneless retinas (Fig. 9*e*), despite the lack of change in the total number of terminations made by these bipolar cells (Fig. 9*c*). We infer this to be a product of larger pedicle-like structures receiving multiple invaginations, as has been shown ultrastructurally for such respecified photoreceptor terminals in the $Nrl^{-/-}$ retina (Strettoi et al., 2004).

Discussion

The present results demonstrate that two different classes of bipolar cell, innervated by the rods or by the cones, differentiate their characteristic dendritic morphologies even when their normal afferent innervation is eliminated or, in the case of the cone bipolar cells, significantly increased. In the conefull retinas, rod bipolar cells build small dendritic arbors that branch repeatedly, stratifying across all depths of the OPL among the terminals of respecified cones. Likewise, the cone bipolar cell retains its characteristic morphology, with several large dendrites emerging from a single stalk and sending smaller terminal branches to the inner edge of the OPL, despite losing its normal afferents in the

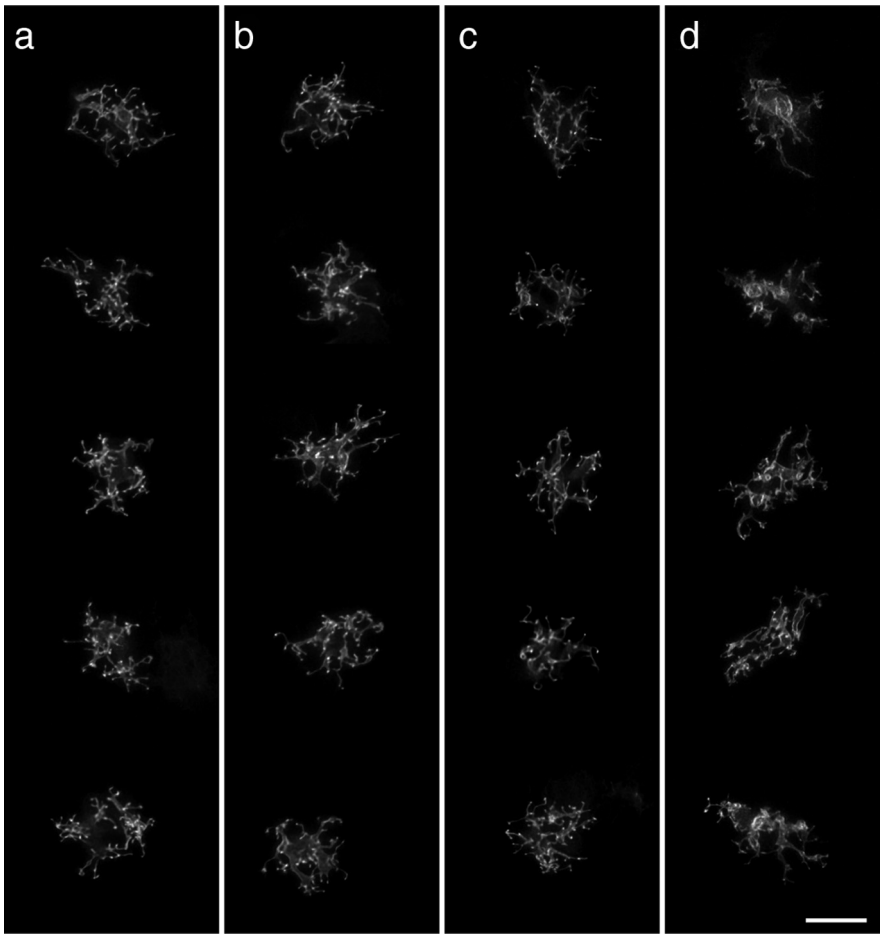

Figure 8. Examples of five rod bipolar cells from wild-type and coneless littermates (***a***, ***b***) and from wild-type and conefull littermates (***c***, ***d***). The dendritic morphology is comparable between wild-type and coneless conditions, but there is a notable absence of puncta at the terminal endings of dendrites in the conefull condition. Scale bar, 10 μm.

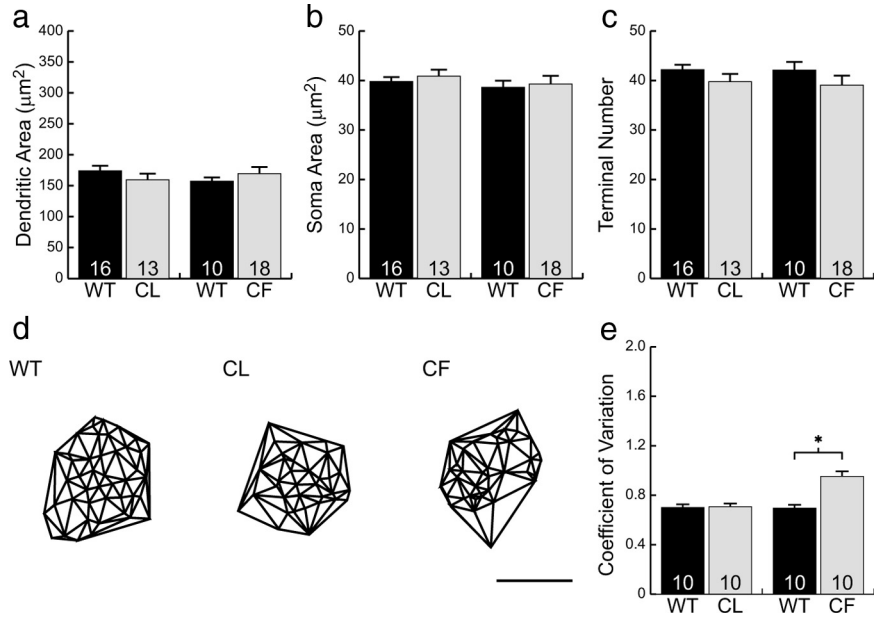

Figure 9. Rod bipolar cell dendritic field size (***a***), soma size (***b***), and the number of terminals per dendritic field (***c***) were not significantly different from wild-type retinas in either the coneless (CL) or conefull (CF) retinas. The Delaunay triangulation of the dendritic field (***d***) showed those in the conefull retina to be significantly more clustered than those in wild-type retinas (***e***). Means and SEs are plotted in each histogram. Scale bar, 10 μm. *$p < 0.01$.

coneless retina and being presented with an almost 20-fold increase of afferents in the conefull retina. It therefore appears that the gross morphology of retinal bipolar cells is likely directed by cell intrinsic factors that control their stratification and branching. The extent of the dendritic fields also did not change, but we cannot rule out a role for homotypic interactions restricting this growth (Wässle et al., 2009). Indeed, occasional cone bipolar cells avoided colonizing pedicles in close proximity to the soma but innervated those farther away (Fig. 2*c–e*). This may reflect the presence of neighboring homotypic cells that colonize such pedicles; alternatively, it may be that such pedicles are associated with the population of true-blue cones and are not innervated by the Type 7/CB4a bipolar cell (Haverkamp et al., 2005).

Not all features of the bipolar cells remain unchanged, however, because a closer examination of the small terminal branches of the dendritic arbor reveals a marked response to variations in the presence of the photoreceptors, particularly the cone bipolar cells. In wild-type retinas, the cone bipolar cell forms clusters of terminal branches only at loci in which cone pedicle active sites reside. When presented with an OPL that lacks these discrete locations, achieved by either removing all of the cones or providing ubiquitous coverage of cone terminals, the cone bipolar cell consistently fails to form such discrete clusters of terminals. The rod bipolar cell also undergoes a slight remodeling of its terminal branches when deprived of its normal afferents, no longer producing characteristic finger-like terminals with bulbous endings that extend vertically but instead forming thick dendrites that give off terminals with smoother, tapered endings that show a tendency for clustering. These results show that bipolar cells depend on their normal afferents to pattern the fine dendritic branches that underlie their connectivity. In each case, however, it is surprising that the total number of terminal endings per dendritic field is conserved, suggesting that this feature of the fine terminal differentiation is also intrinsically defined.

The cone bipolar cells are particularly intriguing, because they normally colonize discrete loci in the OPL in which pedicles are positioned, whereas the rod bipolar cells extend fine branchlets to invade a collection of spherules distributed both across and through much of the thickness of the OPL. The implication for the cone bipolar cell is that it must pro-

duce dendrites that form independent of the afferents (presumably dictated cell intrinsically). In the wild-type retina, these dendrites subsequently target the pedicles based on proximity. This is consistent with the sharp turns exhibited by some of the dendrites in the wild-type retina, as if they detect the location of individual pedicles only as they extend through the local microenvironment. In other cases, they appear to colonize pedicles from adjoining pedicles. This suggests that the presence of pedicles does not induce the formation or initial trajectory of the outgrowing dendrites, and the dendritic fields in the coneless retina would tend to support this; they produce a roughly comparable dendritic field area, yet, failing to detect nearby pedicles, they form single sparse terminals that may be connecting with a subset of rods by default. In the conefull retina, conversely, their relative immunity to the presence of excess cone numbers may be explained by a temporal dependency, with the later-generated (respecified) cones differentiating their terminals in the more outer parts of the OPL too late to influence cone bipolar cell differentiation. Indeed, On bipolar cell dendrites have been shown to exhibit exploratory behavior in postnatal day 5 mouse retinas (Morgan et al., 2006), well before rod spherules invade the OPL, at approximately postnatal day 8 (Sherry et al., 2003). Alternatively, the respecified cones may fail to express genes that play a role in promoting bipolar cell recognition of their pedicles.

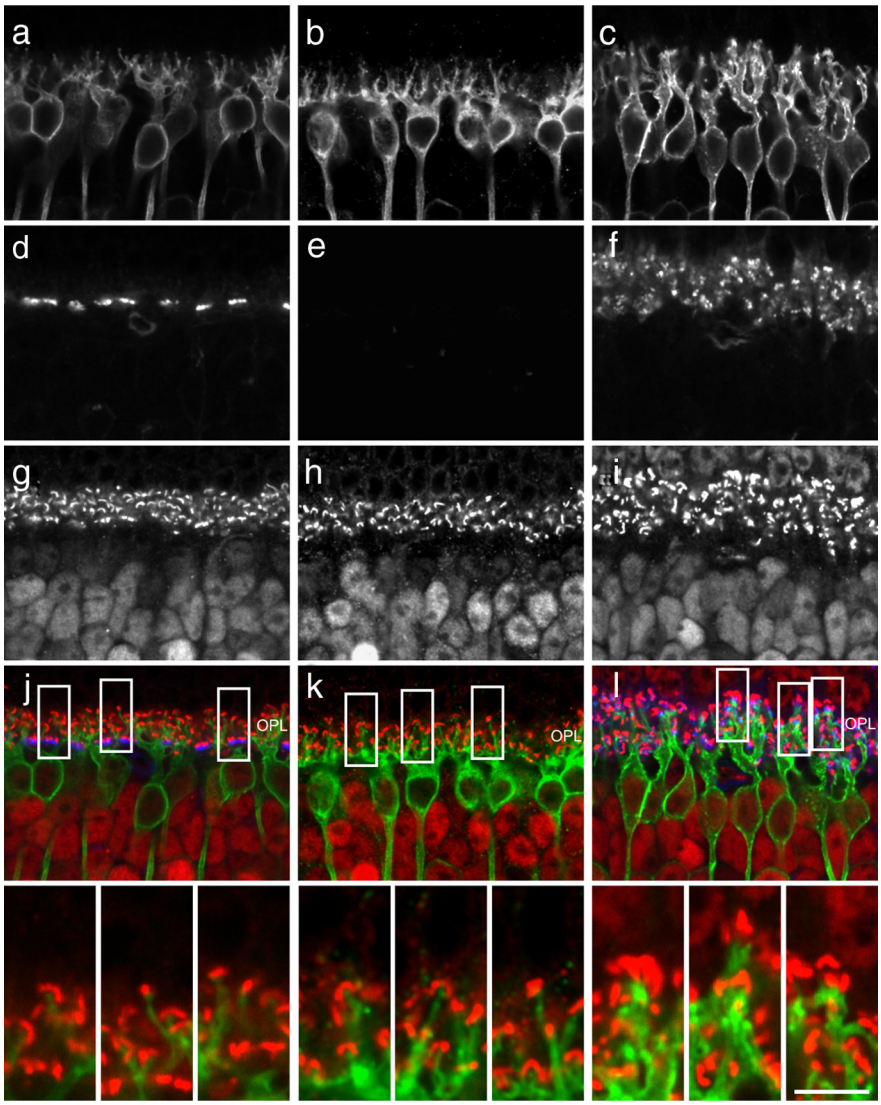

Figure 10. Single optical sections of PKC-labeled rod bipolar cells in wild-type, coneless, and conefull retinas (***a–c***) stained for cone terminals with PNA (***d–f***) and ribbon synapses with CtBP2 (***g–i***), to reveal their relationships in the reorganized OPL of the coneless and conefull retina. Insets show that the dendritic endings of rod bipolar cells at the cone terminals in the conefull retina are adjacent to CtBP2-labeled ribbon synapses (***l***). Note the coarser dendritic stalks that extend into the OPL in the conefull retina (***c***, compare with ***a*** and ***b***). PKC, CtBP2, and PNA channels displayed as green, red, and blue in merged images, but only the PKC and CtBP2 are shown at higher magnification in the insets at the bottom. Scale bar: full images, 15 μm; insets, 5 μm.

The failure of these cells to differentiate normal clusters of terminals in the conefull retina is still surprising. This may indicate that even the earlier generated cones (those that would normally have become cones) are not quite normal in this respecified OPL, consistent with their failure to form a stratum of large pedicles along the inner border of the OPL. However, the retinal horizontal cell, which also receives cone innervation, displays a marked hypertrophy of its dendritic arbor in the conefull retina (Raven et al., 2007), suggesting that the respecified cones in these retinas are competent to increase the growth and elaboration of dendrites. It may be that the cone bipolar cells and the horizontal cells respond differentially to these afferent-derived signals by virtue of their own intrinsic constraints: cone bipolar cells exhibit an intrinsic specification of terminal endings and appear to avoid extending into the outermost portion of the OPL in the conefull retina (present results), whereas the horizontal cells are conspicuously hypertrophic, extending processes throughout the entire dendritic field rather than periodically as clusters, as well as across the full depth of the OPL (Raven et al., 2007).

The rod bipolar cells, in contrast, undergo a change in their morphology in the conefull retina that may simply reflect the different physical constraints imposed therein: the OPL is approximately twice its normal thickness, judging by the distribution of synaptic ribbons (Figs. 6, 10*i*, compare with *g* in each case), and so their longer dendritic course may demand a greater girth of these processes. Within the OPL, the differentiation of terminations associated with these respecified cones may yield differences in the terminal structure of the dendrites, producing less of a bulbous expansion within the photoreceptor terminal, and some degree of clustering by virtue of making multiple connections within individual respecified cone pedicle endings.

In summary, the present analysis has shown that both cone and rod bipolar cells are competent to establish and maintain most features of their dendritic arbors in the absence of their normal afferents. The finer terminal extensions that characterize each of these two bipolar cell types, in contrast, are patterned by the presence of a normal population of afferents in each case: cone bipolar dendritic terminals cluster only the presence of normal cone pedicles, whereas rod bipolar dendritic terminals are uniformly distributed in the presence of a normal population of

rod spherules. The fact that each type of bipolar cell differentiates essentially independent of the presence of its specific afferent population may enable these cells to become connected to the alternative afferent population, given the above cell-intrinsic constraints. Although the molecular mechanisms that regulate afferent-dependent dendritic patterning remain to be determined, the present study makes clear that the control of such patterning is independent from the morphogenetic instructions governing general dendritic growth and branching, themselves likely to be the downstream consequences of cell-intrinsic differentiation programs (Kim et al., 2008).

References

Boycott BB, Wässle H (1991) Morphological classification of bipolar cells of the primate retina. Eur J Neurosci 3:1069–1088.

Chan TL, Martin PR, Grünert U (2001) Immunocytocemical identification and analysis of the diffuse bipolar cell type DB6 in macaque monkey retina. Eur J Neurosci 13:829–832.

Farajian R, Raven MA, Cusato K, Reese BE (2004) Cellular positioning and dendritic field size of cholinergic amacrine cells are impervious to early ablation of neighboring cells in the mouse retina. Vis Neurosci 21:13–22.

Ghosh KK, Bujan S, Haverkamp S, Feigenspan A, Wässle H (2004) Types of bipolar cells in the mouse retina. J Comp Neurol 469:70–82.

Grünert U, Martin PR (1991) Rod bipolar cells in the macaque monkey retina: immunoreactivity and connectivity. J Neurosci 11:2742–2758.

Haverkamp S, Grünert U, Wässle H (2001) The synaptic architecture of AMPA receptors at the cone pedicle of the primate retina. J Neurosci 21:2488–2500.

Haverkamp S, Wässle H, Duebel J, Kuner T, Augustine GJ, Feng G, Euler T (2005) The primordial, blue-cone color system of the mouse retina. J Neurosci 25:5438–5445.

Haverkamp S, Michalakis S, Claes E, Seeliger MW, Humphries P, Biel M, Feigenspan A (2006) Synaptic plasticity in *CNGA3*$^{-/-}$ mice: cone bipolar cells react on the missing cone input and form ectopic synapses with rods. J Neurosci 26:5248–5255.

Haverkamp S, Specht D, Majumdar S, Zaidi NF, Brandstätter JH, Wasco W, Wässle H, Tom Dieck S (2008) Type 4 OFF cone bipolar cells of the mouse retina express calsenilin and contact cones as well as rods. J Comp Neurol 507:1087–1101.

Hopkins JM, Boycott BB (1996) The cone synapses of DB1 diffuse, DB6 diffuse and invaginating midget, bipolar cells of a primate retina. J Neurocytol 25:381–390.

Hopkins JM, Boycott BB (1997) The cone synapses of cone bipolar cells of primate retina. J Neurocytol 26:313–325.

Huang L, Max M, Margolskee RF, Su H, Masland RH, Euler T (2003) G protein subunit Gγ13 is coexpressed with Gαo, Gβ3, and Gβ4 in retinal ON bipolar cells. J Comp Neurol 455:1–10.

Keeley PW, Reese BE (2010) Morphology of dopaminergic amacrine cells in the mouse retina: independence from homotypic interactions. J Comp Neurol. Advance online publication. Retrieved January 19, 2010. doi: 10.1002/cne.22270.

Keeley PW, Whitney IE, Raven MA, Reese BE (2007) Dendritic spread and function coverage of starburst amacrine cells. J Comp Neurol 505:539–546.

Kim DS, Matsuda T, Cepko CL (2008) A core paired-type and POU homeodomain-containing transcription factor program drives retinal bipolar cell gene expression. J Neurosci 28:7748–7764.

Lin B, Masland RH (2005) Synaptic contacts between an identified type of ON cone bipolar cell and ganglion cells in the mouse retina. Eur J Neurosci 21:1257–1270.

Liu X, Grishanin RN, Tolwani RJ, Rentería RC, Xu B, Reichardt LF, Copenhagen DR (2007) Brain-derived neurotrophic factor and TrkB modulate visual experience-dependent refinement of neuronal pathways in retina. J Neurosci 27:7256–7267.

Mariani AP (1981) A diffuse, invaginating cone bipolar cell in primate retina. J Comp Neurol 197:661–671.

Mataruga A, Kremmer E, Müller F (2007) Type 3a and type 3b OFF cone bipolar cells provide for the alternative rod pathway in the mouse retina. J Comp Neurol 502:1123–1137.

Mears AJ, Kondo M, Swain PK, Takada Y, Bush RA, Saunders TL, Sieving PA, Swaroop A (2001) Nrl is required for rod photoreceptor development. Nat Genet 29:447–452.

Morgan JL, Dhingra A, Vardi N, Wong RO (2006) Axons and dendrites originate from neuroepithelial-like processes of retinal bipolar cells. Nat Neurosci 9:85–92.

Pignatelli V, Strettoi E (2004) Bipolar cells of the mouse retina: a gene gun, morphological study. J Comp Neurol 476:254–266.

Poché RA, Raven MA, Kwan KM, Furuta Y, Behringer RR, Reese BE (2008) Somal positioning and dendritic growth of horizontal cells are regulated by interactions with homotypic neighbors. Eur J Neurosci 27:
1607–1614.

Raven MA, Reese BE (2003) Mosaic regularity of horizontal cells in the mouse retina is independent of cone photoreceptor innervation. Invest Ophthalmol Vis Sci 44:965–973.

Raven MA, Oh EC, Swaroop A, Reese BE (2007) Afferent control of horizontal cell morphology revealed by genetic respecification of rods and cones. J Neurosci 27:3540–3547.

Reese BE, Raven MA, Stagg SB (2005) Afferents and homotypic neighbors regulate horizontal cell morphology, connectivity and retinal coverage. J Neurosci 25:2167–2175.

Rich KA, Zhan Y, Blanks JC (1997) Migration and synaptogenesis of cone photoreceptors in the developing mouse retina. J Comp Neurol 388:47–63.

Sherry DM, Wang MM, Bates J, Frishman LJ (2003) Expression of vesicular glutamate transporter 1 in mouse retina reveals temporal ordering in development of rod vs. cone and ON vs. OFF circuits. J Comp Neurol 465:
480–498.

Soucy E, Wang Y, Nirenberg S, Nathans J, Meister M (1998) A novel signaling pathway from rod photorecptors to ganglion cells in mammalian retina. Neuron 21:481–493.

Strettoi E, Pignatelli V, Rossi C, Porciatti V, Falsini B (2003) Remodeling of second-order neurons in the retina of rd/rd mutant mice. Vis Res 43:867–877.

Strettoi E, Mears AJ, Swaroop A (2004) Recruitment of the rod pathway by cones in the absence of rods. J Neurosci 24:7576–7582.

Telkes I, Lee SC, Jusuf PR, Grünert U (2008) The midget-parvocellular pathway of the marmoset retina: a quantitative light microscopic study. J Comp Neurol 510:539–549.

Tian N, Copenhagen DR (2003) Visual stimulation is required for refinement of ON and OFF pathways in postnatal retina. Neuron 39:
85–96.

Tsukamoto Y, Morigiwa K, Ueda M, Sterling P (2001) Microcircuits for night vision in mouse retina. J Neurosci 21:8616–8623.

Tsukamoto Y, Morigiwa K, Ishii M, Takao M, Iwatsuki K, Nakanishi S, Fukuda Y (2007) A novel connection between rods and ON cone bipolar cells revealed by ectopic metabotropic glutamate receptor 7 (mGluR7) in mGluR6-deficient mouse retinas. J Neurosci 27:6261–6267.

Wässle H, Puller C, Müller F, Haverkamp S (2009) Cone contacts, mosaics and territories of bipolar cells in the mouse retina. J Neurosci 29:106–117.

Whitney IE, Raven MA, Ciobanu DC, Williams RW, Reese BE (2009) Multiple genes on chromosome 7 regulate dopaminergic amacrine cell number in the mouse retina. Invest Ophthalmol Vis Sci 50:1996–2003.

Yamagata M, Sanes JR (2008) Dscam and Sidekick proteins direct lamina-specific synaptic connections in vertebrate retina. Nature 451:465–469.

Young HM, Vaney DI (1991) Rod-signal interneurons in the rabbit retina. 1. Rod bipolar cells. J Comp Neurol 310:139–153.